Electronic properties calculation of MgO thin films adsorbed on semi-infinite Ag(001)

G. Butti,[1,2,*] M. I. Trioni,[2] and H. Ishida[3]
[1]*Dipartimento di Scienza dei Materiali, Università di Milano-Bicocca, Via Cozzi 53, 20125 Milano, Italy*
[2]*Istituto Nazionale per la Fisica della Materia-UdR Milano Bicocca, Via Cozzi 53, 20125 Milano, Italy*
[3]*College of Humanities and Sciences, Nihon University, Sakura-josui, Tokyo 156, Japan*
(Received 8 July 2004; published 17 November 2004)

We report a theoretical investigation of the electronic structure of ultrathin MgO films on Ag(001). Such a study has been motivated by recent experiments in which a peculiar behavior was observed when the film thickness is less than a few layers, suggesting that the interface properties may play a crucial role. We tried to verify such a statement by a comparative analysis between the clean surfaces of Ag and MgO, and the 1-, 2-, and 3-monolayer (ML) adsorbed systems. To perform these calculations we applied the embedding method {proposed by Inglesfield [J. E. Inglesfield, J. Phys. C **14**, 3795 (1981)]} which allows us to consider a semi-infinite substrate and is therefore one of the state-of-the-art methods for the theoretical treatment of surfaces. We find evidences of a weak interaction between the silver substrate and the MgO overlayers and we show how, as the film thickness exceeds the 2 ML width, the electronic properties converge on those of a clean MgO surface. In the last part of the work we also suggest a possible interpretation of the ultraviolet photoelectron spectroscopy data obtained on these systems.

DOI: 10.1103/PhysRevB.70.195425 PACS number(s): 73.20.At, 73.20.Hb

I. INTRODUCTION

Thin oxide films on metal substrates are nowadays a matter of growing technological interest.[1] Their employment as insulator layers in micro- and nanodevices has driven a considerable effort to further understand the interface properties of these systems.[2,3] In particular, for magnesium oxide film, evidences of interesting properties such as an enhanced reactivity,[4] or a peculiar behavior in electron emission[5] were found in the ultrathin limit (1–3 atomic layers). These features indicate that, in this thickness range, the metallic substrate plays an active role on the supported MgO film, modifying its electronic properties. Furthermore, it has been shown that the nonordinary behavior is enhanced at the single monolayer (ML) coverage.[4,6,7] In this paper we focus on MgO/Ag(001), a system for which *layer-by-layer* growth occurs producing a very regular film, as shown by scanning tunneling microscopy (STM).[6,8] This is possible because of the small lattice mismatch ($\sim$2.9%) between the bulk silver lattice parameter and the MgO one, which allows epitaxial growth. Despite the considerable number of experimental studies focusing on this system, some results are still matter of discussion. To our knowledge, the theoretical investigation performed so far went more in the direction of determining the equilibrium structure of the system, obtaining a nice agreement with experimental data.[9] The necessary and natural extension of these studies concerns the determination of a detailed picture of the electronic properties of the MgO/Ag(001) interface and represents the main purpose of this work. We apply the embedding method, originally developed by Inglesfield[10] to the treatment of surfaces; within this framework, differently with respect to more widely used approaches as supercell or slab methods, one is able to consider the real semi-infinite nature of the silver substrate.[11,12]

This paper is organized as follows: in Sec. II we briefly decribe our computational technique, reporting also the values of the main parameters present in the calculation. In Sec. III we briefly analyze the electronic properties of the clean Ag(001) surface in order to build a reference for the subsequent treatment of more complex systems. In Sec. IV we consider the MgO monolayer on Ag(001) system; we show the results regarding the density of states (DOS), comparing it to the one obtained for a free-standing MgO layer, and we characterize some of the surface intrinsic features. In Sec. V we then compare results obtained for the single layer with those obtained for 2 and 3 ML of MgO/Ag(001); in this way we are able to highlight the features in the MgO layer due to the interaction with the Ag substrate. It should also help in sketching how the electronic properties vary as a function of the film thickness, aligning progressively with MgO surface properties; in Sec. VI, the metal induced gap states (MIGS) are also considered. Finally, in Sec. VII we focus on the unexpected ultraviolet photoelectron spectroscopy (UPS) results obtained by Altieri *et al.*,[4] proposing an interpretation for them. Section VIII is devoted to the conclusions.

II. COMPUTATIONAL FRAMEWORK

By the embedding method we consider a surface taking into account its intrinsic feature represented by the semi-infinite bulk substrate below it. We partition the space into three different volumes, considering a surface region embedded between the bulk substrate region and the vacuum one; the boundaries between these volumes are called embedding surfaces. This kind of calculation requires a multistep procedure, necessary in order to determine the ground state Green's function in the surface region. We must first calculate the bulk Green's function, in order to produce, in the second step, an embedding potential which will replace the bulk substrate in the self-consistent surface calculation performed in the final step. The embedding potential replacing the vacuum region is instead evaluated analytically, as de-

TABLE I. Calculated structural parameters for bulk Ag. V_0, the equilibrium atomic volume, B, the bulk modulus, and B', are the parameters obtained from the Murnaghan equation of state.

	a (Å)	B (Mbar)	V_0 (Å^3)	B'	χ^2
This work	4.089	1.080	17.09	5.50	$<10^{-12}$
Experiment	4.085[14]	1.087[15,a]	17.162[16]	⋯	⋯

[a]Extrapolated at 0 K.

scribed in Ref. 12. Once in possession of the Green's function for the embedded surface region we can calculate the local DOS, $\sigma(\mathbf{r},E)=(1/\pi)\Im mG(\mathbf{r},\mathbf{r},E+i\delta)$, which can be integrated over an energy range to obtain the charge density $n(\mathbf{r})$. It should be noted that most of the DOSs we present in this work are calculated with a small but finite imaginary part of the energy, δ, in order to be able to detect discrete features using afinite mesh sampling the energy axis. For a detailed explanation of the embedding method see Refs. 10–12. Our calculations are based on a full-potential linearized augmented plane wave (FLAPW) scheme; the embedded region is partitioned into muffin-tins (MT) spheres and an interstitial region. The embedding surface on the bulk side has a bumpy shape which allows one to include in the embedding region the whole MT spheres of interface atoms, avoiding a possible source of inaccuracy. The main parameters that we must set for the Green's function expansion are the cutoff momentum of the plane wave basis, $|\mathbf{k}|=[\mathbf{k}_\parallel^2+k_z^2]^{1/2}$, where the z axis is chosen as the surface normal, and the maximum angular momentum inside the MT spheres, $l_{\max}$. The first quantity which define the plane-wave energy cutoff is fixed to 10.24 Ry, while the second is chosen as $l_{\max}=9$. The other parameters which have to be set concern the geometry of the embedded region: the MT radii are $r_{\mathrm{MT}}^{\mathrm{Ag}}=2.65$ a.u. and $r_{\mathrm{MT}}^{\mathrm{O}}=r_{\mathrm{MT}}^{\mathrm{Mg}}=1.70$ a.u.; the embedded region extends for 25 a.u. in the z direction and the surface Brillouin zone (SBZ) was sampled by a 10×10 regular mesh consisting in 100 $\mathbf{k}_\parallel$ points of which 21 are independents. All the results presented in this paper are obtained within the local density approximation (LDA) for the exchange and correlation energy.[13]

III. CLEAN Ag(001) SURFACE

In order to calculate the embedding potential replacing the bulk Ag substrate, we determined the bulk electronic structure and we also performed some tests on the accuracy of our computational scheme, determining the equilibrium lattice parameter a and the bulk modulus B. The results we obtained are in excellent agreement with experimental data, as reported in Table I. The bulk band structure and density of states also reproduce the results already present in literature.[17]

In order to build a solid basis for the subsequent overlayer calculations, we studied the clean Ag(001) surface with some detail. We included the two topmost atomic layers in the surface embedded region; this is a realistic approximation, at least for metals where there is a very high screening efficiency.

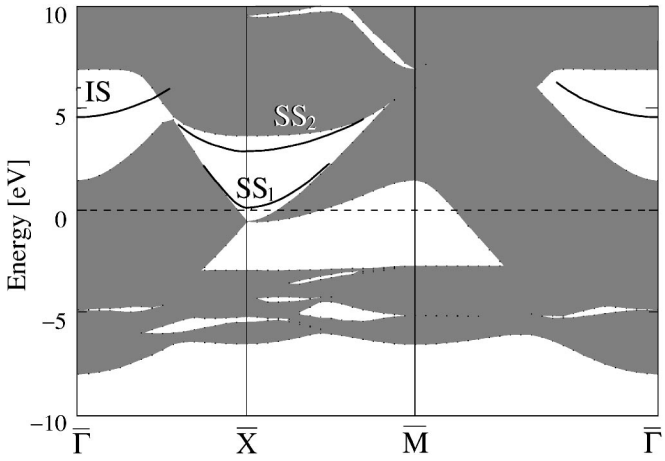

FIG. 1. Surface band structure for Ag(001).

We consider first the projection of bulk band structure onto the SBZ relative to the (001) surface shown in Fig. 1. In this way one can identify intrinsic surface features, distinguishing them from bulk ones; let us remark that the availability of a continuous DOS is a very powerful tool to resolve surface structures, differentiating between discrete surface states and states propagating into the bulk.

We characterized the discrete states shown in Fig. 1 by calculating their energy and effective mass. The data we obtained are reported in Table II. For what concerns states SS_1 and SS_2 our results are in good agreement with experimental ones, as well as with ones obtained in previous theoretical calculations. In particular state SS_2 was observed at 3.5 ± 0.2 eV in inverse photoemission experiments byAltmann *et al.*[18] while electroreflectance measurements by Kolb *et al.*[19] indicated a slightly lower energy, of about 3.1 eV. The density functional theory (DFT)-LDA calculation, reported in Ref. 20, determined an energy of 2.99 eV. For what concerns state SS_1, it could be put in relationship with state B in the work by Kolb *et al.* which is located slightly below the Fermi level (~-0.1 eV). In our calculation this state is empty, at an energy of 0.15 eV, in perfect agreement with previous result.[20] States SS_1 and SS_2, in correspondence of the $\bar{X}$ point, display opposite bonding character: SS_1 presents charge density maxima between the atoms while in the same positions there are minima (nodal planes) for the antibonding SS_2 state. In both cases, their charge distribution is essentially located on the surface layer. For what concerns state IS we observed that its charge density has maximum further outside the topmost layer, as it is typical of states induced by the image potential at metal surfaces (image states). Al-

TABLE II. Effective mass and spectral position of the main intrinsic features of Ag(001) surface.

State	Effective mass (m_e)	Energy (eV)
SS_1	$\bar{X}-\bar{M}$:0.52	0.15
SS_2	$\bar{X}-\bar{\Gamma}$:0.56	2.88
IS	0.99	4.52 (-0.17[a])

[a]With respect to the vacuum level E_v, reported in Table III

though the asymptotic dependence of the potential is not correct within the LDA, because it does not reproduce the $-1/4z$ decay of the image potential, it is well known that the potential in the immediate neighborhood of the surface can allow one to describe in a very approximate way the first image state in the Rydberg series. The effective mass we obtained for this state is 0.99 m_e, in perfect agreement with the experimental value of 0.98 ± 0.02 m_e, obtained by Ferrini *et al.*[21] On the contrary, the locality of the LDA functional does not allow us to reproduce the correct spectral position of this state, and therefore the energy we obtain, −0.17 eV, is quite different from the experimental value of -0.53 ± 0.05 eV.

IV. MONOLAYER COVERAGE

We now consider one monolayer of MgO adsorbed on the Ag(001) surface. The monolayer system was reproduced using a 1×1 unit cell; this choice is supported by STM images showing that, at least locally, the experimental samples present a very regular morphology.[6,8]

In order to determine the equilibrium structure of the MgO film we performed some calculations using different plane-wave pseudopotential (PW-PP) codes; in fact total energy minimization is a hard task to perform within a FLAPW framework. Moreover the final result should not differ significantly being bond lengths in solids essentially determined by valence wave functions which are correctly described in a PW-PP approach. The two equilibrium structures we obtained present some small differences one respect to the other but they all were in substantial agreement with previous theoretical determinations.[9] However the nice agreement found in Ref. 9 between theoretical and experimental results induced us to adopt the calculated coordinate set reported in that work. In the equilibrium configuration the oxygen atoms are on top of the silver ones, while the magnesium ones are located in a four fold hollow position with respect to the Ag layer. The independent optimization of the z coordinates of the Mg and O atoms has clarified that the equilibrium geometry corresponds to an arrangement in which the Mg atoms are located slightly closer to the silver layer than the O ones displaying a rumpling of about 0.15 Å. This feature is also present in the case of the MgO/Pd(111) interface where a rumpling of 0.16 Å is reported by Giordano *et al.*[7] Based on these conclusions, we model the MgO monolayer system for the electronic structure calculations enclosing two silver layers and a MgO one in the embedded region. In Fig. 2, we report the layer-resolved DOS, plotting separately the contribution of the MT volumes (thicker lines) and that of the interstitial region pertaining to the layer (thinner lines). Being Ag and MgO closed-packed materials, the contribution from the MT volumes is clearly dominant. The DOSs in panel (a) refer to the most external silver layer in the monolayer system (continuous line) and in the case of a clean Ag(001) surface (dashed line). The reference energy is the Fermi level of bulk silver. We note that the greater modification as a consequence of the adsorption of the MgO layer is the appearance of a large shoulder in correspondence of the highest peaks in the MgO valence DOS, reported in panel

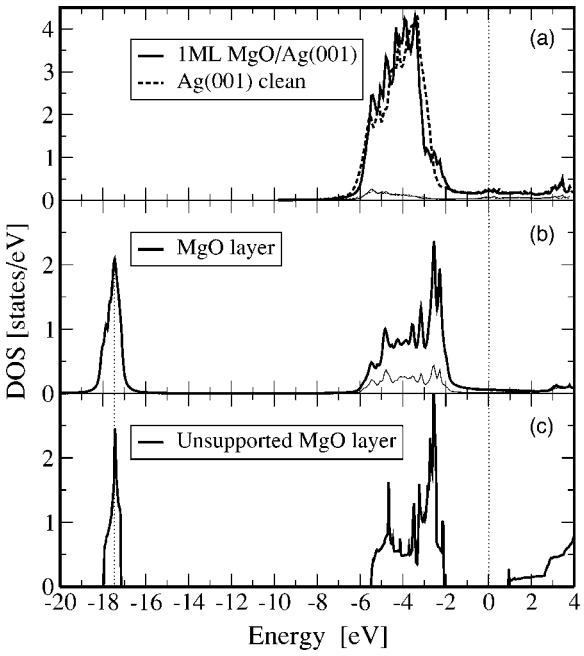

FIG. 2. Density of states in the MgO and top Ag layers. The energy axis scale is referred to the Fermi level of bulk silver. Thicker lines refers to MT volumes, while thinner ones indicate contribution from interstitial region. (a) The topmost Ag layer in the case of an Ag(001) clean surface and in the 1 ML MgO/Ag(001) system. (b) The MgO layer in the 1 ML MgO/Ag(001) system. (c) Unsupported MgO(001) layer.

(b). The interstitial part is instead very similar in both cases: these states seem to be left unmodified by the adsorption of the MgO layer. In order to better understand the features in the MgO DOS due to the presence of the metal substrate, we report in panel (c) the DOS of an unsupported MgO layer calculated using the periodic supercell (non-embedding) version of our code. Being that the Fermi level is undefined in the case of an unsupported monolayer, we chose to align these two DOS according to the 2s peaks, located between −18 and −17 eV, which are quite sharp and narrow. In the supported case the peak is slightly wider, indicating a greater dispersion of the 2s states for the supported MgO layer. Let us remark that the Lorentzian tails of the peaks in the supported case are a spurious feature due to the small imaginary part of the energy. The two 2p bands are quite similar in their shape; the most interesting feature is represented by the presence, in the case of the supported MgO layer, of a considerable amount of states crossing the Fermi level, and connecting the valence with the conduction band. This density of states is thought to be originated from an hybridization with silver sp band[4] and it is not present in the unsupported MgO layer, where we observe the typical gap of this material, even if its amplitude is not correctly estimated within DFT.[22] These states are usually referred to as MIGS[2,3,23] and are a general feature of metal-ceramic interfaces. In a different picture, they could also be seen as states originated by metal wave functions which become evanescent functions when they enter the oxide, damping roughly exponentially with distance.

In order to better understand the nature of the MgO valence band we calculate the $\mathbf{k}_\parallel$-resolved DOS. In this way we

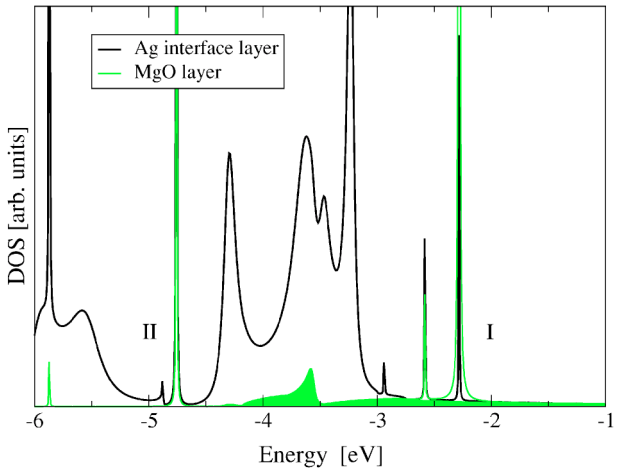

FIG. 3. (Color online) Valence band DOS at $\bar{\Gamma}$ for the 1 ML MgO/Ag(001). The shaded region represents the continuous part in the MgO layer DOS.

are able to distinguish between MgO $2p$ states which hybridize with the substrate, falling in the energy range of the Ag band and those which keep their discrete nature falling in an energy range where there are no silver states suitable for hybridization. In particular, we calculate the DOS at $\bar{\Gamma}$ point, with a very small imaginary part of the energy (1.5×10^{-3} eV) and a very dense sampling focusing only on the valence band range. In Fig. 3 we report the DOSs relative to the Ag interface layer and to the MgO one. We identify three main discrete structures: one at −4.75 eV, labeled as structure II, one at −2.6 eV and one at −2.25 eV, labeled as structure I. The peak at −2.6 eV simply represents the tail of a surface feature of the Ag substrate and therefore does not play any particular role in the interface properties. Beside these peaks there is also a continuous part of the DOS, starting from −4.5 eV and extending until 1.5 eV, which we highlighted by the gray (green) shaded region. This continuous DOS was determined by performing a calculation in which the imaginary part of the Green's function is equal to zero; on the real axis discrete states are delta functions and therefore cannot be revealed sampling the energy axis with a finite mesh. In order to better understand the nature of the discrete states, we calculated the charge distribution corresponding to structures I and II. At this particular point of the SBZ, we obtain a charge density distribution, which is strongly reminiscent of atomic orbitals. These densities are shown in Fig. 4; the charge corresponding to the peak at −2.25 eV (structure I) is essentially parallel to the surface plane; for this reason we would refer to it as the $p_{\|}$ state. The other peak of interest, the one at −4.75 eV has a charge distribution which resembles very much the p_z orbital in the isolated atom picture; for this reason we refer to it as a p_z state, even if this definition is inappropriate. The $p_{\|}$ state lies completely outside the Ag d band; the p_z, instead, falls exactly in a sort of microgap of Ag band where we also find a discrete state in Ag DOS. The charge density relative to these last two states is equally distributed on the MgO and on the interface Ag layer, originating an interface state.

On the other hand, the continuous DOS represents O $2p$ states hybridized with the Ag sp band, the ones which could

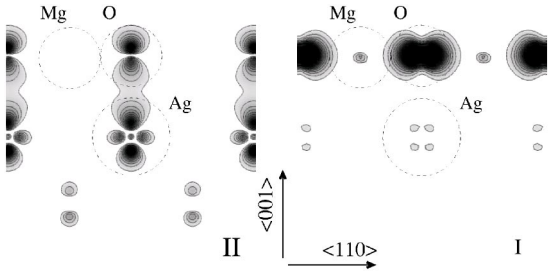

FIG. 4. Charge density plot relative to regions I and II in Fig. 3. The darker regions correspond to higher charge densities.

be identified as MIGS. This statement is supported by several reasons; first of all the energy range in which the hybrid states exist is more or less the same as that of the sp band. Moreover, the shape of the DOS on the MgO layer is the same as we obtain by summing s and p component in the Ag layer DOS. These states are the less localized ones and therefore they are the most suitable for the propagation-hybridization process into the MgO layer.

V. 2 AND 3 ML COVERAGE

In this section, we study the electronic properties of the 2 and 3 ML MgO films; in particular, we are interested in determining how the properties observed for the monolayer are modified for higher thicknesses. In this way we could determine a sort of "critical thickness" characterizing the ultrathin limit, distinguishing this class of materials from those displaying common insulator properties, where the substrate has no active role. The first step in such analysis is the comparison between the DOSs in the 2 and 3 ML systems and the ones calculated for a clean MgO(001) surface. Results are shown in Fig. 5; panels (a), (b), and (c) refer to the 2 and 3 ML systems, the former corresponding to the continuous lines and the latter to the dashed ones. In particular panel (a) contains results for the interface Ag layer, while (b) and (c) those of the interface and top MgO layer respectively. Comparing the DOS in the first three panels, there is no evidence suggesting that the electronic properties of the 2 ML system should differ significantly from those of the 3 ML. Indeed both the interface and the top MgO DOS are very similar and also the two interface Ag layer do not present strong differences. Only in the energy region around the Fermi level, the amount of MIGS is considerably larger for the top MgO layer in the 2 ML case with respect to the 3 ML one. Being this quantity of the order of 0.02 states/eV, this feature is not visible in Fig. 5, and will be treated in detail in the next section.

In panel (d) we report the DOS for the top layer of the clean MgO(001) surface. The similarity between this DOS and that of the top MgO layer in the 3 ML system supports the idea that the electronic properties of the film are already converged to those of a clean MgO surface. An additional point of view in this respect can be achieved analyzing the variation of the work function in the systems considered. To avoid misunderstandings in dealing with a metallic/insulator hybrid system such as ours, we define the work function as

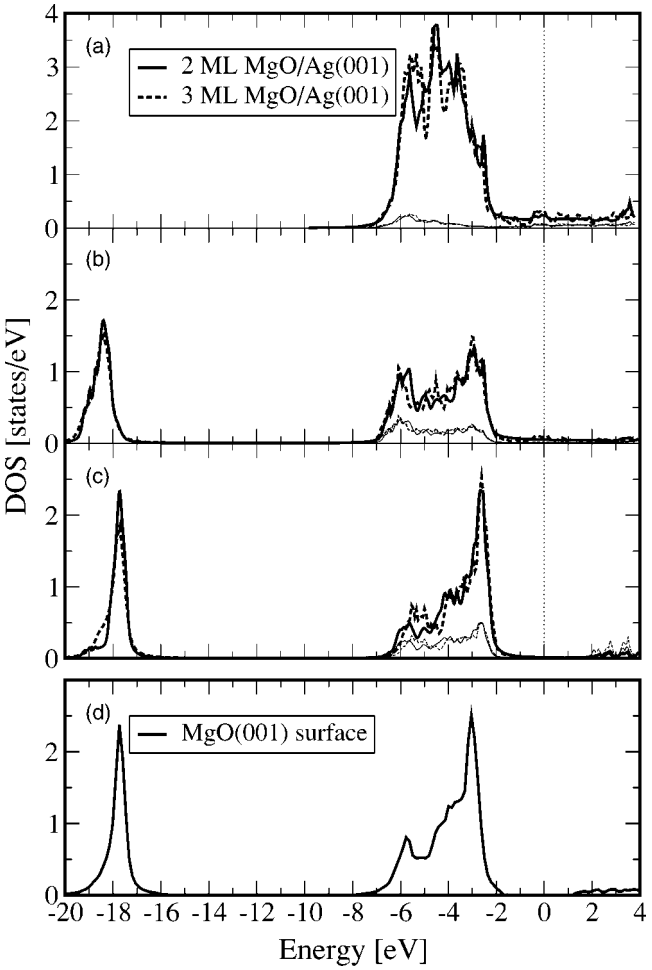

FIG. 5. Comparison of the DOSs of 2 and 3 ML [panels (a), (b), and (c)] system with the DOS of the top layer of the clean MgO(001) surface [panel (d)]. Thicker lines refer to MT volumes, while thinner ones indicate contribution from interstitial region. (a) Interface Ag layer; (b) interface MgO layer; (c) top MgO layer; (d) top MgO layer in a MgO(001) clean surface.

the energy of the vacuum level with respect to the Fermi one of bulk silver. The results are reported in Table III and display a decrease of the work function with the increase of MgO film thickness. However, if we consider the DOSs, reported in Fig. 5(c), we notice that on the external MgO layer,

TABLE III. Work function for Ag(001) and 1, 2, and 3 ML of MgO/Ag(001).

System	Calculated (eV)	Measured (eV)
Clean Ag(001)	4.69	4.22±0.04[24]
1 ML MgO/Ag(001)	3.98	···
2 ML MgO/Ag(001)	3.34	···
	5.4±0.1[a]	
3 ML MgO/Ag(001)	3.37	···
	5.4±0.1[a]	
MgO(001) clean surface	5.45[a]	6.7±0.4[25]

[a]Distance from top of valence band to the vacuum level.

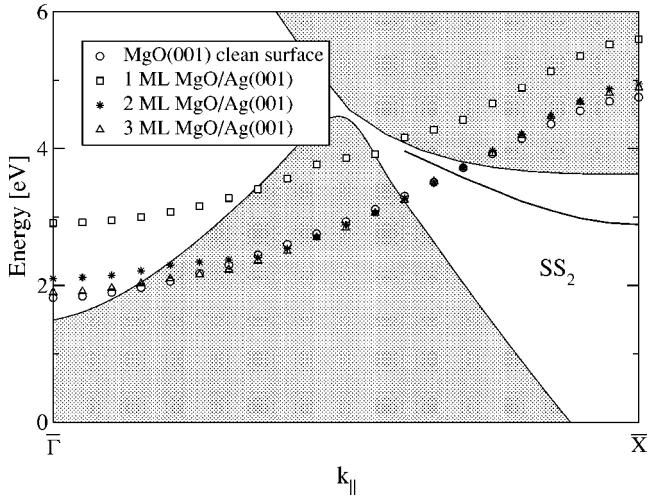

FIG. 6. MgO surface state dispersion in the $\bar{\Gamma}$-$\bar{X}$ path. The shaded regions represent Ag bands projection, while the continuous line reproduces Ag surface state SS_2.

the number of states at the Fermi level is close to zero. As the thickness of the MgO slab increases, the reference energy should be therefore set at the top of the MgO valence band. The value obtained in this way, both for the 2 and 3 ML case, is very close to the calculated one for the clean MgO surface, confirming the idea that already in this thickness range these systems have similar properties. Further evidence is found analyzing the dispersion along the $\bar{\Gamma}$-$\bar{X}$ path of the MgO empty surface state which is present in all the surfaces terminated with a MgO layer. The dispersion of this surface state is plotted in Fig. 6 over the projection of Ag bands; SS_2 refers to the silver surface state discussed in Sec. III. We note that only for the monolayer the energy of this state is significantly (of about 1 eV) different with respect to the other systems. In the 2 ML its dispersion is very similar to the one of a clean MgO surface and, for the 3 ML MgO slab, the peak positions nearly coincide. In order to better understand the electronic structure of the thicker MgO film we calculate the DOS in the 3 ML system at $\bar{\Gamma}$ with the same detailed level used to obtain Fig. 3. The results obtained are shown in Fig. 7; the lines and areas drawn in light gray (green) correspond to the discrete and continuous structures of the top MgO layer while the ones in dark gray (blue) refer to the MgO interface layer. We also report the DOS in the Ag interface layer which is useful to understand which states interact more with the overlayer. We note that the structures that we have labeled as I and II in Fig. 3 are still present and do not differ very much with respect to our previous determination. In particular, structure I (~ -2 eV) is slightly shifted toward higher energies and corresponds to $p_{\|}$ states located only in the outermost MgO layer. The element arising from this analysis is the detection of the continuous $2p$ band, originated by the interaction between $2p$ O states located in different layers. The edge of this band is around -3.1 eV, in agreement with the experimental results by Tjeng *et al.*,[26] for the clean MgO surface. Let us remark that the $p_{\|}$ state is shifted toward higher energies in consequence of the shift in the Madelung field due to the lower coordina-

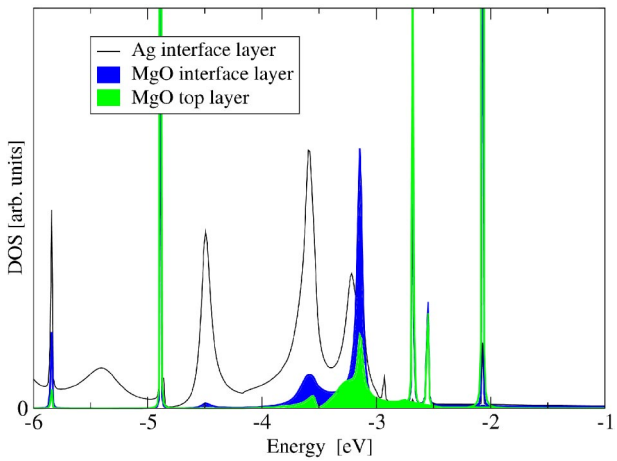

FIG. 7. (Color online) Valence band DOS at $\bar{\Gamma}$ for the 3 ML MgO/Ag(001).

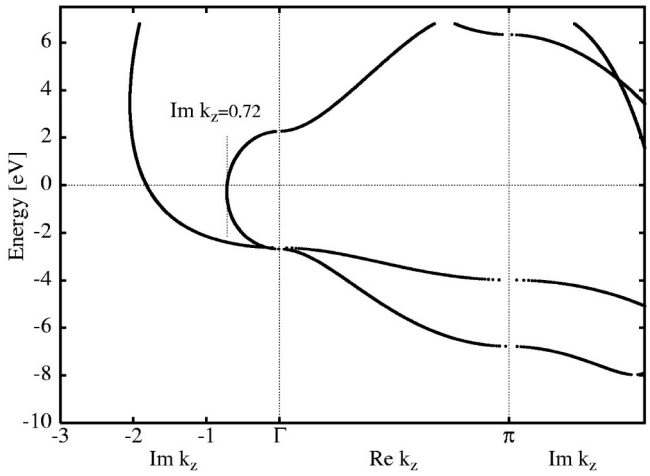

FIG. 8. MgO complex band structure at $\bar{\Gamma}$ using $1/d$ units. In the middle part of the plot we report the solution with real values of k_z. In the side regions the solutions with purely imaginary values of k_z (left side) or with $\Re e k_z = \pi/d$ (right side) are plotted.

tion of the surface layer, falling outside the band and becoming a discrete surface state. In particular it presents the feature typical of a Tamm state, i.e., a flat dispersion, following the band edge.

VI. MIGS CHARACTERIZATION

In order to obtain a more complete description of the MgO/Ag(001) system, we report here a more detailed picture of the MIGS-related features. As already pointed out by Bordier and Noguera,[23] MIGS are characterized by a typical damping length. Note that this quantity depends on the energy of the states themselves: at the insulator midgap this value is minimum while close to the band edges the wave functions are weakly damped. The analysis we present here is focused at the Ag substrate Fermi level, which corresponds to an energy very close to the middle of MgO gap. A first, rough, estimate of the damping length is made by determining the values of the maxima of the oscillating charge density as a function of penetration distance z. We performed this analysis on the 3 ML system, in order to have access to the largest data set. We then fit our data with an exponentially decaying function: $\rho(z) = \alpha \exp(-2kz)$. The value of the parameter k determined from this fit is equal to 0.21 a.u., i.e., $0.84/d$, where d is the interplanar distance. Consequently the decaying length for the wave functions is equal to 1.19 d. We can compare these results, with a more sophisticated method making use of MgO complex band structure. This means calculating $E(k_z)$ for bulk MgO solutions at a given $k_\parallel$; when these solution sare real, wave functions oscillate and propagate through the solid. On the contrary, the region in which they are complex is the gap region; wave functions at these energy values are not allowed to propagate, being evanescent solutions. The damping factor of these kind of solutions (which are the ones giving rise to the MIGS phenomenon) is given by the value of imaginary part of k_z. An overall view of this concept as well as of the method used to calculate such band structure is reported in Ref. 27. In Fig. 8 we report the results obtained for MgO, computed at $\bar{\Gamma}$ point where we show the determination of the damping length. The solution corresponds to $\Im m k_z = 0.72/d$, in substantial agreement with the previous determination. The discrepancy is due to the fact that within this complex band structure framework we are considering how wave functions decay into an infinitely thick bulk MgO. This is, however, a reasonable approximation and the agreement between the two estimates demonstrates that in this case finite size effects are not fundamental.

VII. COMPARISON WITH EXPERIMENTAL RESULTS: VALENCE BAND STRUCTURE AROUND THE FERMI LEVEL

In this section we give an interpretation to the UPS data obtained by Altieri *et al.*[4] for the MgO monolayer system. In the performed experiment, they recorded an UPS spectra on a freshly grown sample using a He I source (21.2 eV), at normal emission with respect to the surface. The same investigation was done, as a comparison, on the clean Ag(001) surface. In the energy range from −3.5 eV to the Fermi level, they obtained a higher signal for the monolayer system than for the clean silver surface. This result, i.e., the increase of the number of states around the Fermi level after the growth of an insulator layer over a metal, is somewhat surprising and constitutes one of the features which attracted attention on this class of compounds. We then tried to analyze this result comparing our DOS with the valence band spectra; these two objects are obviously not the same but within a zeroth order approximation they can be thought as one proportional to the other. Moreover, using He I radiation, Ag 4d states and O 2p ones have equal cross section for the UPS,[28] suggesting that when performing the experiment on the clean surface and on the 1 ML MgO/Ag(001) the sampled volume is more or less the same. With these premises, the result we obtain integrating over the whole SBZ is in contrast with the experiment because the DOS on the MgO layer is smaller than that on any Ag layer [see Figs. 2(a) and 2(b)]. This

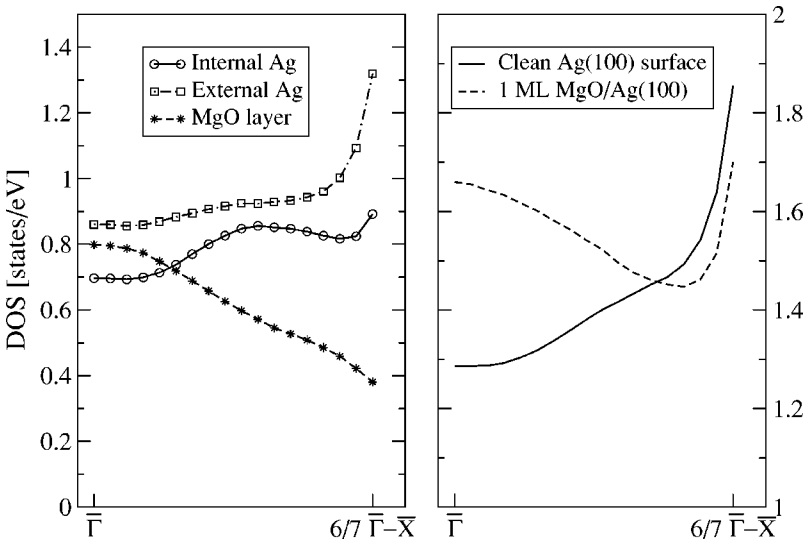

FIG. 9. Variation of the DOS as a function of $\mathbf{k}_{\|}$. The panel on the left displays the result relative to each layer in the 1 ML system while in the one on right we report the comparison between the 1 ML system and the clean Ag(001) surface, obtained summing the DOS in the two topmost layers of each system.

result also confirms what has been obtained in Ref. 6 but does not lead to a further comprehension of this phenomenon. A different point of view can be achieved if we introduce in our analysis the fact that, in the photoemission experiment, the electrons collected are those emitted along the direction normal to the surface sample; in this way only a reduced portion around $\bar{\Gamma}$ point of the SBZ is sampled.[29] Our comparison should therefore be made integrating over the same small portion of SBZ. Within this frame we get a result which is in agreement with the experimental one, obtaining a DOS which is higher for the 1 ML MgO system than for the Ag clean surface in the proximity of the Fermi level. To better display the results of this analysis we plotted in Fig. 9 the DOS as a function of the value of $\mathbf{k}_{\|}$ at a fixed energy. In particular we chose to report the values for $E=E_F$ but we verified that the same behavior is observed elsewhere in the energy range under analysis. We also excluded the zone border $(\bar{X})$ from the plot because the presence in that point of a surface state could affect the comprehension of the general meaning of the plot. In the left panel we report the DOS values for the monolayer while in the right one we show two curves, obtained by summing the DOS of the first and second surface layer in two systems: the Ag clean surface and the monolayer one. The overall result is quite self-explaining: the most important feature is that the great majority of MgO states is located near the zone center and their number decreases as we go toward the zone border. The opposite trend is shown by silver states which in both plots are in greater number near the zone boundary. A spectroscopy which samples a limited portion near the SBZ center will then emphasize the states belonging to the MgO layer, underestimating the ones from the silver substrate. This could be the reason of the unexpected result obtained by experimentalists and could be definitely proved by performing the same experiment collecting the electrons emitted at a grazing angle with respect to the surface.

VIII. CONCLUSIONS

In this work we analyzed the electronic properties of ultrathin MgO films adsorbed on a Ag(001) substrate, describing the features due to the interactions in this metal/metal-oxide interface. Taking advantages of our embedding approach we achieved a detailed description of the electronic structure in each of these systems, in particular for what concerns the discrete surface and interface states. The results obtained allow us to speculate about the transition between the Ag surface and the pure MgO one, in terms of the number of MgO monolayers grown on the metal substrate. In the monolayer limit, we observed the known hybridization between the Ag *sp* band and the O 2*p* one, resulting in the presence of a continuum of states in the MgO gap (MIGS). The propagation of these states is characterized by an exponential decay: therefore the amount of these states on the surface is much reduced as the MgO film thickness increases. The DOS on the top layer of a 3 ML MgO film does not present any difference with respect to the one of the top layer of a clean MgO(001) surface. This fact, together with the analysis of the work function variation and of the dispersion of the unoccupied MgO surface state indicates a rapid convergence, in terms of the film thickness, of the film electronic properties to the MgO surface ones. These results strongly support the idea that the mutual interaction is localized at the interface layers and therefore features due to such interaction appear enhanced in the monolayer regime and might influence the surface reactivity. We also studied the propagation of MIGS, determining the damping length of these states into the MgO film; we obtained a substantial agreement between two different method of calculating this quantity. Finally, we analyzed the results of Altieri *et al.*[4] and we interpret the measured UPS spectra around the Fermi level in the monolayer regime. The great majority of the states responsible for the detected signal are confined in a reduced portion of SBZ, where the number of hybridized states is greater than it is in the rest of reciprocal space, as shown by our calculation.

ACKNOWLEDGMENTS

The authors are grateful to G. Pacchioni, for suggesting to them the topic of this work together with S. Valeri, S. Altieri, and L. Giordano for very useful discussions.

*Electronic address: gabriele.butti@unimib.it

[1] S. A. Chambers, Surf. Sci. Rep. **39**, 105 (2000).
[2] M. W. Finnis, J. Phys.: Condens. Matter **8**, 5811 (1996).
[3] C. Noguera, *Physics and Chemistry at Oxide Surfaces* (Cambridge University Press, Cambridge, 1996).
[4] S. Altieri, L. H. Tjeng, and G. A. Sawatzky, Phys. Rev. B **61**, 16 948 (2000).
[5] Y. T. Matulevich, T. J. Vink, and P. A. Zeijlmans van Emmichoven, Phys. Rev. Lett. **89**, 167601 (2002).
[6] S. Schintke, S. Messerli, M. Pivetta, F. Patthey, L. Libioulle, M. Stengel, A. De Vita, and W. D. Schneider, Phys. Rev. Lett. **87**, 276801 (2001).
[7] L. Giordano, J. Goniakowski, and G. Pacchioni, Phys. Rev. B **67**, 045410 (2003).
[8] S. Valeri, S. Altieri, U. del Pennino, A. di Bona, P. Luches, and A. Rota, Phys. Rev. B **65**, 245410 (2002).
[9] C. Giovanardi, A. di Bona, T. S. Moia, S. Valeri, C. Pisani, M. Sgroi, and M. Busso, Surf. Sci. **505**, L209 (2002).
[10] J. E. Inglesfield, J. Phys. C **14**, 3795 (1981).
[11] H. Ishida, Phys. Rev. B **63**, 165409 (2001).
[12] H. Ishida, Surf. Sci. **388**, 73 (1997).
[13] J. P. Perdew and A. Zunger, Phys. Rev. B **23**, 5048 (1981).
[14] L. Liu and W. A. Bassett, J. Appl. Phys. **44**, 1475 (1973).
[15] D. R. Smith and F. R. Fickett, J. Res. Natl. Inst. Stand. Technol. **100**, 119 (1995).
[16] R. W. Cahn, P. Haasen, and H. W. King, *Physical Metallurgy: Structure of Pure Metals* (Elsevier, Amsterdam, 1983).
[17] V. L. Moruzzi, J. F. Janak, and A. R. Williams, *Calculated Electronic Properties of Metals* (Pergamon, Oxford, 1978).
[18] W. Altmann, V. Dose, and A. Goldmann, Z. Phys. B: Condens. Matter **65**, 171 (1986).
[19] D. M. Kolb, W. Boeck, K. M. Ho, and S. H. Liu, Phys. Rev. Lett. **47**, 1921 (1981).
[20] L. Savio, L. Vattuone, M. Rocca, V. De Renzi, S. Gardonio, C. Mariani, U. del Pennino, G. Cipriani, A. Dal Corso, and S. Baroni, Surf. Sci. **486**, 65 (2001).
[21] G. Ferrini, C. Giannetti, D. Fausti, G. Galimberti, M. Peloi, G. P. Banfi, and F. Parmigiani, Phys. Rev. B **67**, 235407 (2003).
[22] M. Lannoo, M. Schlüter, and L. J. Sham, Phys. Rev. B **32**, 3890 (1985).
[23] G. Bordier and C. Noguera, Phys. Rev. B **44**, 6361 (1991).
[24] M. Chelvayohan and C. H. B. Mee, J. Phys. C **15**, 2305 (1982).
[25] L. N. Kantorovich, A. L. Shlugher, P. Sushko, J. Gunster, P. Starcke, D. W. Goodman, and V. Kempter, Faraday Discuss. **144**, 173 (1999).
[26] L. H. Tjeng, A. R. Vos, and G. A. Sawatzky, Surf. Sci. **235**, 269 (1990).
[27] D. Wortmann, H. Ishida, and S. Blügel, Phys. Rev. B **65**, 165103 (2002).
[28] http://ulisse.elettra.trieste.it/elements/webelements.html
[29] M. C. Desjonqueres and D. Spanjaard, *Concepts in Surface Physics: Appendix F3* (Springer, Berlin, 1998).